EUKARYOTIC CELL, Nov. 2008, p. 1888–1894 Vol. 7, No. 11
1535-9778/08/$08.00+0 doi:10.1128/EC.00194-08


# ESCRT-III Protein Snf7 Mediates High-Level Expression of the *SUC2* Gene via the Rim101 Pathway▽

Peter Weiß,[1] Stefanie Huppert,[2] and Ralf Kölling[1]*

*Institut für Lebensmittelwissenschaft und Biotechnologie, Fg. Gärungstechnologie, Universität Hohenheim, D-70599 Stuttgart, Germany,[1] and Artes Biotechnology GmbH, D-40764 Langenfeld, Germany[2]*

Received 13 June 2008/Accepted 9 September 2008

**The yeast (*Saccharomyces cerevisiae*) Snf7 family consists of six highly charged, coiled-coil-forming proteins involved in multivesicular body (MVB) formation. Although all proteins perform a common function at late endosomes, individual mutants also show distinct phenotypes. This suggests that Snf7 homologues have additional functions separate from their role in MVB formation. In this report, we explored the molecular basis for the *s*ucrose-*n*on*f*ermenting phenotype of *snf7* mutants. Our Northern blotting experiments provide evidence that Snf7 is involved in the regulation of *SUC2* transcription. The Snf7-dependent regulation of *SUC2* transcription does not appear to involve the transcription factor Mig1, since Mig1 phosphorylation after glucose derepression was not affected in a Δ*snf7* mutant. Instead, we show that Snf7 influences *SUC2* expression by regulating the level of the transcription factor Nrg1. Snf7 exerts its effects on Nrg1 levels through activation of the transcription factor Rim101, which is part of the yeast alkaline response pathway ("Rim101 pathway"). This is supported by the findings that deletion of *RIM101* or overexpression of *NRG1* from the *ADH1* promoter leads to the same *SUC2* expression level as deletion of *SNF7*. In addition, deletion of other components of the Rim101 pathway, like *RIM13* and *RIM20*, led to the same growth phenotype on raffinose media as deletion of *SNF7*. Furthermore, Snf7 turned out to be dispensable for *SUC2* expression in an *NRG1* deletion background. Thus, the effects of Snf7 on *SUC2* expression can be completely accounted for by its effect on Nrg1 levels.**

The class E vacuolar protein sorting (Vps) proteins are involved in the formation of vesicles that bud into the interior of late endosomes forming a multivesicular body (MVB) (18). Endocytic cargo is incorporated into these vesicles. When the MVB fuses with the vacuole, the vesicles are released into the vacuolar lumen and proteins contained in the vesicles are degraded. Class E proteins have been grouped into three protein complexes, ESCRT-I, -II and -III, associated with the endosomal membrane (22). It is thought that these complexes act consecutively in cargo recruitment and MVB vesicle formation. The ESCRT-III complex consists of four proteins: Did4/Vps2, Snf7/Vps32, Vps20, and Vps24/Did3. The ESCRT-III proteins are part of a protein family of highly charged coiled-coil-forming proteins with six members in yeasts (1, 6, 8). The two members of this family (Did2/Vps46, Mos10/Vps60) that have not been mapped to ESCRT-III are class E proteins as well and are also required for late endosome function.

Here, we focus on the Snf7 protein. Originally, this protein was identified in a screen for mutants defective for growth on sucrose as a carbon source (*snf* represents *s*ucrose *n*on*f*ermenting) (15). The enzyme invertase encoded by the *SUC2* gene is required for sucrose utilization. *SUC2* is expressed under low-glucose conditions and repressed by high glucose. Most of the *snf* mutants isolated in the screen turned out to be defective for invertase derepression under low-glucose conditions. Two classes of Snf proteins could be distinguished: proteins involved in glucose signaling (Snf1 and -4) (7) and proteins that are part of the Swi-Snf chromatin-remodeling complex (Snf2, -5, -6, and -11) (29). Two additional Snf proteins, Snf7 and Snf8/Vps22 (a component of ESCRT-II), are found among the collection of class E Vps functions. How the *snf* phenotype is related to the endosomal function of these proteins is unclear.

By genome-wide screening (mostly two-hybrid screens), several proteins interacting with Snf7 have been identified. One interaction partner is the class E Vps protein Bro1/Vps31, which appears to act late in the MVB pathway, probably after or at the level of ESCRT-III (17, 19). Bro1 seems to coordinate the deubiquitination of endocytic cargo proteins by recruiting the deubiquitinating enzyme Doa4 to endosomes (13). Another interaction partner is the Bro1 homologue Rim20. Rim20 is one of the components of the Rim101 pathway that is involved in the transcriptional response to alkaline pH (30). Despite the homology to Bro1, Rim20 does not appear to have an endosomal function. In addition to Rim20, a further component of the Rim101 pathway, Rim13, a calpain-like cysteine protease, interacts with Snf7. Further interaction partners are Vps20, which forms a subcomplex of ESCRT-III with Snf7, and Vps4, an AAA ATPase involved in disassembly of ESCRT complexes at endosomes (3).

The six proteins of the Snf7 family are all required for late endosome function, yet mutants of individual members of this family have distinct phenotypes (8). This points to additional nonendosomal functions for these proteins. We analyzed the role of Snf7 in expression of the glucose-repressed *SUC2* gene. We found that Snf7 affects *SUC2* transcription at a step after

* Corresponding author. Mailing address: Institut für Lebensmittelwissenschaft und Biotechnologie, Fg. Gärungstechnologie (150f), Universität Hohenheim, Garbenstr. 23, D-70599 Stuttgart, Germany. Phone: 49-711-459 22310. Fax: 49-711-459 24121. E-mail: koelling@uni-hohenheim.de.

▽ Published ahead of print on 19 September 2008.

TABLE 1. Yeast strains used in this study

| Strain[a] | Genotype | Source |
|---|---|---|
| JD52 | *MAT***a** *his3-Δ200 leu2-3,112 lys2-801 trp1-Δ63 ura3-52* | J. Dohmen, Cologne, Germany |
| JD116 | Δ*doa4*::*LEU2* | J. Dohmen, Cologne, Germany |
| RKY1511 | Δ*vps4*::*HIS3* | This study |
| RKY1654 | Δ*mos10*::*HIS3* | This study |
| RKY1728 | Δ*did2*::*HIS3* | This study |
| RKY1730 | Δ*vps24*::*HIS3* | This study |
| RKY1732 | Δ*did4*::*HIS3* | This study |
| RKY1828 | Δ*did4*::*kanMX* Δ*vps24*::*HIS3* | This study |
| RKY1829 | Δ*snf7*::*HIS3* Δ*vps20*::*kanMX* | This study |
| RKY1835 | Δ*did2*::*HIS3* Δ*mos10*::*kanMX* | This study |
| RKY1852 | Δ*snf7*::*TRP1* | This study |
| RKY1853 | Δ*vps20*::*TRP1* | This study |
| RKY1876 | Δ*vps27*::*kanMX* | This study |
| RKY1922 | Δ*bro1*::*kanMX* | This study |
| RKY2058 | *MIG1*::13 myc-*HIS3* | This study |
| RKY2100 | Δ*rim20*::*kanMX* | This study |
| RKY2102 | Δ*rim13*::*kanMX* | This study |
| RKY2104 | Δ*snf7*::*kanMX MIG1*::13 myc-*HIS3* | This study |
| RKY2175 | Δ*rim101*::*HIS3* | This study |
| RKY2176 | *NRG1*::*3HA-HIS3* | This study |
| RKY2180 | Δ*snf7*::*TRP1 NRG1*::*3HA-HIS3* | This study |
| RKY2206 | Δ*nrg1*::*HIS3* | This study |
| RKY2207 | Δ*snf7*::*TRP1* Δ*nrg1*::*HIS3* | This study |
| RKY2208 | *ADH1p-3HA*::*NRG1*::*HIS3* | This study |
| RKY2284 | Δ*rim13 NRG1*::*3HA-TRP1* | This study |
| RKY2285 | Δ*rim20 NRG1*::*3HA-TRP1* | This study |
| RKY2286 | Δ*rim101 NRG1*::*3HA-TRP1* | This study |

[a] All strains were derived from JD52.

Mig1 inactivation and mediates its effects on *SUC2* via the Rim101 pathway.

## MATERIALS AND METHODS

**Yeast strains.** The yeast (*Saccharomyces cerevisiae*) strains used are listed in Table 1. Deletion strains and strains carrying tagged gene variants were derived from the wild-type strain, JD52. They were constructed by one-step gene replacement with PCR-generated cassettes (12). The deletions and insertions were verified by PCR.

**Phosphatase treatment.** Cells were grown overnight to exponential phase (optical density at 600 nm [$OD_{600}$] of <0.8 [$5 \times 10^7$/ml]) in YPD (yeast extract, peptone, dextrose) medium. Cells at an $OD_{600}$ of 4 were pelleted and heated at 95°C for 5 min. After resuspension in 100 μl sodium dodecyl sulfate (SDS) gel sample buffer (2% SDS, 10% glycerol, 60 mM Tris-Cl [pH 6.8], 0.1% bromphenol blue, 20 mM dithiothreitol), the cells were broken by agitation with glass beads for 5 min at 4°C and then centrifuged for 5 min at 500 × *g* to remove cell debris. The supernatant was diluted 1:5 with 60 mM Tris-Cl (pH 6.8). An aliquot corresponding to an $OD_{600}$ of 2 of cells was incubated with 5 U calf intestine phosphatase for 4 h at 37°C. The control samples without phosphatase were treated in the same way. After addition of 1 volume of 2× SDS gel sample buffer, the samples were heated again for 5 min at 95°C and then loaded onto the gel.

**Preparation of cell extracts for Western blotting.** Cells were grown overnight to exponential phase ($OD_{600}$ of <0.8 [$5 \times 10^7$/ml]) in YPD medium. Cells at an $OD_{600}$ of 4 were pelleted, washed in cold 10 mM $NaN_3$, and then resuspended in 100 μl cold lysis buffer (50 mM HEPES, 0.3 M sorbitol, 10 mM $NaN_3$, pH 7.5, plus protease inhibitor cocktail). Cells were broken by agitation with glass beads for 5 min at 4°C. After addition of 1 volume of 2× SDS gel sample buffer, proteins were solubilized at 50°C for 15 min. Cell debris was removed by a 13,000 × *g* spin for 2 min in a tabletop centrifuge. An aliquot corresponding to an $OD_{600}$ of cells of 0.2 was loaded onto a SDS-polyacrylamide gel electrophoresis gel and examined by Western blotting.

**Northern blotting.** For RNA isolation, cells were grown overnight to exponential phase ($OD_{600}$ of <0.8 [$5 \times 10^7$/ml]) in YPD medium. Cells at an $OD_{600}$ of 4 were harvested and resuspended in 200 μl extraction buffer (0.5 M NaCl, 0.2 M Tris-Cl [pH 7.6], 10 mM EDTA, 1% SDS). After addition of 400 mg glass beads and 200 μl of a 1:1 mixture of phenol-chloroform, the samples were vortexed for 2.5 min. Then 300 μl extraction buffer and 300 μl phenol-chloroform were added and the samples were vortexed again for 1 min. After 5 min of centrifugation in a tabletop centrifuge at full speed, the aqueous phase was recovered and reextracted with 1 volume of phenol-chloroform. The aqueous phase was mixed with 2 volumes of ethanol and spun for 10 min at full speed. The pellet was washed two times with 3 M Na-acetate (pH 6) to remove DNA, washed with 1 ml 70% ethanol, and finally resuspended in 100 μl sterile $H_2O$. The RNA was separated on a formaldehyde agarose gel, blotted to a GeneScreen Plus membrane (Perkin Elmer, Boston, MA), and hybridized to specific DNA probes according to the instructions of the manufacturer. Autoradiograms were scanned, and the signal intensities were quantified with the program ImageJ (http://rsbweb.nih.gov/ij/). *SUC2* signals were normalized to the actin signal.

**Invertase assay.** Yeast cells grown overnight to the exponential phase ($OD_{600}$ of <0.8 [$5 \times 10^7$/ml]) in YPD plus 5% glucose at 25°C were harvested, washed in $H_2O$, and resuspended in YPD plus 0.1% glucose. At time intervals after the shift to low glucose, cell extracts were prepared and invertase activity was determined. For determination of invertase activity, cells at an $OD_{600}$ of 1 were harvested, washed twice in 10 mM $NaN_3$, and resuspended in 100 μl 0.1 M Na-acetate (pH 5). After breakage of the cells by glass beading for 5 min, 150 μl 0.1 M Na-acetate (pH 5) was added and cell debris was removed by centrifugation at 500 × g for 5 min. Five microliters of the supernatant was mixed with 100 μl 0.1 M Na-acetate (pH 5) and 25 μl of freshly prepared 0.5 M sucrose and incubated for 20 min at 37°C. The reaction was stopped by the addition of 150 μl 0.2 M $K_2HPO_4$ and heating at 95°C for 3 min. After cooling on ice, 1 ml reaction mix (2.5 mg/ml glucose oxidase, 0.5 mg/ml peroxidase, 0.3 mg/ml *o*-dianisidine, 0.1 M K phosphate [pH 7]) was added. After incubation at 37°C for 30 min, the reaction was stopped by the addition of 6 M HCl and the $A_{540}$ was measured in a spectrophotometer.

## RESULTS

**Deletion mutants of *SNF7* family members show distinct phenotypes.** The Snf7 family proteins perform a function at late endosomes, probably as part of a larger protein complex (1, 2, 8). The phenotypes of *SNF7* family member mutants, however, suggested that these proteins carry out additional functions. To investigate this more systematically, deletion mutants of all six *SNF7* family members were examined for their growth phenotypes under conditions that activate different cell signaling pathways (Fig. 1). Cells were incubated at elevated temperature (37°C) to test for a role in heat shock signaling. To see whether the Snf7 homologues are involved in glucose derepression, glucose-grown cells were spotted onto plates containing raffinose as the sole carbon source. Cells that are defective in glucose derepression, as suggested previously for *snf7* mutants, cannot grow on raffinose and on other carbon sources whose utilization is prevented by the presence of high concentrations of glucose in the growth medium. Also, cells were spotted onto plates containing the cell-wall-disturbing agent Congo red and onto plates containing caffeine. Both Congo red and caffeine activate the Slt2–mitogen-activated protein (MAP) kinase cell integrity pathway (23).

Deletion mutants of the four Snf7 homologues that were assigned to the ESCRT-III complex (Did4, Snf7, Vps20, and Vps24) resembled each other in that they were all sensitive to high temperature (37°C) and 10 mM caffeine. However, in addition, these mutants also showed distinct growth phenotypes: the Δ*snf7* and Δ*vps20* mutants grew poorly on raffinose but were unaffected by Congo red (Fig. 1A), whereas the opposite was true for the Δ*did4* and Δ*vps24* mutants (Fig. 1B). A completely different pattern of growth phenotypes was observed for the deletion mutants of the other two Snf7 homo-

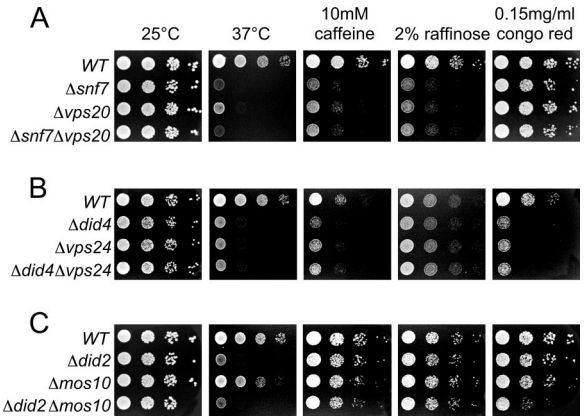


FIG. 1. Growth phenotypes of *SNF7* family deletion mutants. Tenfold serial dilutions of overnight cultures of different yeast strains grown in YPD medium were spotted onto YPD plates containing 10 mM caffeine, 2% raffinose as the sole carbon source (plus 2 μg/ml antimycin), or 0.15 mg/ml Congo red, as indicated. Plates were incubated at 25°C, except for one set of plates that were incubated at 37°C. The following strains were used (from top to bottom): (A) JD52 (wild type [WT]), RKY1852 (Δ*snf7*), RKY1853 (Δ*vps20*), RKY1829 (Δ*snf7* Δ*vps20*); (B) JD52 (WT), RKY1732 (Δ*did4*), RKY1730 (Δ*vps24*), and RKY1828 (Δ*did4* Δ*vps24*); and (C) JD52 (WT), RKY1728 (Δ*did2*), RKY1654 (Δ*mos10*), and RKY1835 (Δ*did2* Δ*mos10*).

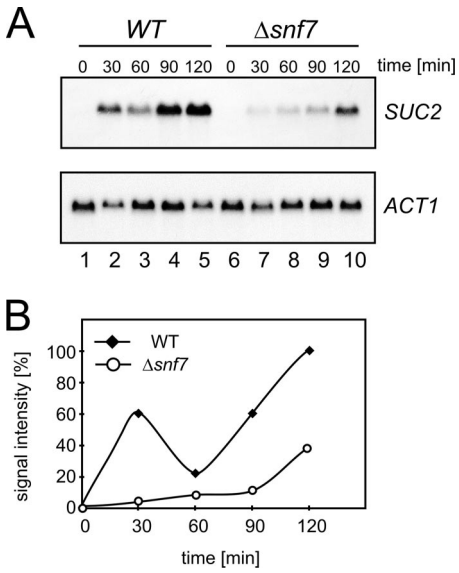


FIG. 2. Effect of Δ*snf7* on invertase expression. (A) Northern blotting. JD52 (wild type [WT], lanes 1 to 5) and RKY1852 (Δ*snf7*, lanes 6 to 10), pregrown in YPD medium (plus 5% glucose), were transferred to low-glucose medium (0.1%). At time zero, RNA was prepared at time intervals after the shift to low glucose (as indicated) and examined for the amounts of *SUC2* (upper panel) and *ACT1* mRNA (lower panel) by Northern blotting with specific DNA probes. (B) Quantification of the Northern blot signals. Closed diamonds, JD52 (WT); open circles, RKY1852 (Δ*snf7*). The *SUC2* signals were normalized to the *ACT1* signals.

logues that have not been mapped to the ESCRT-III complex. While the Δ*mos10* strain grew like the wild type under all conditions tested, the only phenotype observed for the Δ*did2* strain was temperature sensitivity.

Interestingly, two each of the ESCRT-III mutants (Δ*snf7*/Δ*vps20* and Δ*did4*/Δ*vps24*) showed exactly the same pattern of growth phenotypes. This is in line with earlier observations that Snf7/Vps20 and Did4/Vps24 form subcomplexes of the ESCRT-III complex (2). The pairwise identity of growth phenotypes suggests that the two proteins of each subcomplex perform a common function. If this notion is correct, the double-deletion mutant of one pair should show the same phenotype as the single mutants. This is what we observed. In contrast, the Δ*did2* Δ*mos10* double mutant showed a synthetic growth phenotype not observed with the single mutants, i.e., sensitivity to Congo red. This suggests that these two proteins are not part of a common subcomplex but instead perform parallel functions.

**Role of Snf7 in *SUC2* expression.** The phenotypes of the Snf7 family deletion mutants suggest that these proteins perform additional functions unrelated to their role in MVB formation. To explore this nonendosomal function in more detail, we focused on the role of Snf7 in invertase expression. Invertase is required for the utilization of carbon sources like sucrose and raffinose. Its expression from the *SUC2* gene is under glucose control: *SUC2* is expressed on low-glucose media and repressed on high-glucose media. Snf7 is somehow involved in high-level expression of *SUC2* (27, 28). However, how Snf7 participates in *SUC2* expression has not been thoroughly investigated so far.

Several possibilities are conceivable: Snf7 could directly affect transcription of the *SUC2* gene, or it could affect later steps that lead to expression of invertase activity (like nuclear export of mRNA, translation, or transport and turnover of invertase). To see whether Snf7 acts at the transcriptional or posttranscriptional level, Northern blot experiments were performed. Cells were pregrown under repressing conditions (5% glucose) and were then shifted to inducing medium (0.1% glucose). At time intervals after a shift to low-glucose medium, RNA was prepared and examined by Northern blotting for the amount of *SUC2* mRNA. In the wild-type strain, an increase in the amount of *SUC2* mRNA was observed during the time course of the experiment (2 h) (Fig. 2A). In the Δ*snf7* strain, *SUC2* mRNA also increased but to a much lower level. The amount of actin mRNA (*ACT1*) was not affected by the glucose shift, and the amounts were the same in both strains. This experiment shows that Snf7 affects transcript levels and that it is required for full derepression of the *SUC2* gene after the shift to low-glucose medium.

Quantification of the Northern blot signals revealed that the *SUC2* expression profile was biphasic (Fig. 2B). After an initial increase, *SUC2* transcript levels drop and then rise again. A similar observation has been described before (5). It appears that the *SNF7* deletion mainly affects the initial burst of *SUC2* transcriptional activity, since the amount of *SUC2* transcript at later time points was comparable to that of the wild type. The reason for this behavior is at present unclear.

Under high-glucose conditions, expression of the *SUC2* gene is prevented by the Mig1 repressor, which binds to the *SUC2* promoter (14). When the glucose concentration drops to low levels, the Snf1 kinase is activated, which in turn inactivates the Mig1 repressor through phosphorylation (26). Snf7 could interfere at several steps with this signaling cascade. To see whether the glucose-signaling cascade is intact in the Δ*snf7*

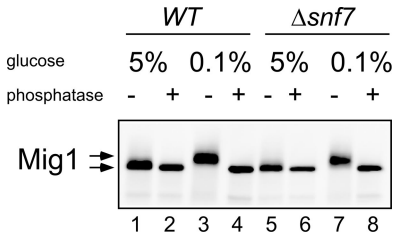


FIG. 3. Mig1 phosphorylation. RKY2058 (wild type [WT], lanes 1 to 4) and RKY2104 (Δ*snf7*, lanes 5 to 8) expressing a 13-Myc-tagged Mig1 variant from the chromosomal copy of the gene were pregrown in YPD medium with 5% glucose. Half of the cells were transferred to low-glucose medium (0.1%) for 1 h, while the other half were further incubated with 5% glucose. Equal amounts of cell extracts were examined for Mig1 phosphorylation by Western blotting with anti-myc antibodies. +, samples treated with phosphatase (even lanes); −, untreated samples (odd lanes).

mutant, we examined whether Mig1 is still phosphorylated after the shift to low-glucose medium. For detection, Mig1 was marked with a 13-Myc tag. After the shift to low glucose, more slowly migrating Mig1 species were observed on Western blots that were condensed to a sharp band that migrated slightly faster by phosphatase treatment (Fig. 3). Both wild-type and Δ*snf7* strains showed the same phosphorylation pattern. This suggests that the glucose-signaling cascade resulting in phosphorylation of Mig1 is still intact in the Δ*snf7* mutant. Thus, Snf7 appears to be involved in a step independent of Mig1 inactivation.

**Effect of class E *vps* mutants on *SUC2* expression.** We were interested to see whether the function of Snf7 in *SUC2* expression is tied to a functional Vps pathway. Therefore, several class E *vps* mutants were tested for growth on raffinose plates (Fig. 4). At least one member each of the different ESCRT complexes was included in the analysis (22). Lack of growth on raffinose was observed for *vps23* (ESCRT-I), *snf8* (ESCRT-II), *snf7*, and *vps20* (ESCRT-III) and *doa4*. A partial growth defect was seen for Δ*vps27* (ESCRT-0) and *bro1*. Basically, the data indicate that the ESCRT complexes functioning upstream of Snf7 are required for growth on raffinose medium. Among the ESCRT-III proteins, only Vps20, which forms a subcomplex with Snf7 (2), is required for growth on raffinose, while the other members of the complex are dispensable. Downstream functions, like *bro1* and *vps4*, also do not seem to be crucial for *SUC2* expression. However, some exceptions from this scheme were noted: Vps37, another subunit of ESCRT-I, was not required for growth on raffinose and Vps27, a component of ESCRT-0, was only partially required. On the contrary, the deubiquitinating enzyme Doa4, which is recruited to late endosomes by Bro1 and which is involved in deubiquitination of endocytic cargo proteins (1, 13, 16), appears to be essential for invertase expression. Since the deubiquitinating activity of Doa4 at endosomes is dependent on Bro1 and since deletion of *BRO1* has only a moderate effect on raffinose growth, the Δ*doa4* effect is probably unrelated to the endosomal function of Doa4.

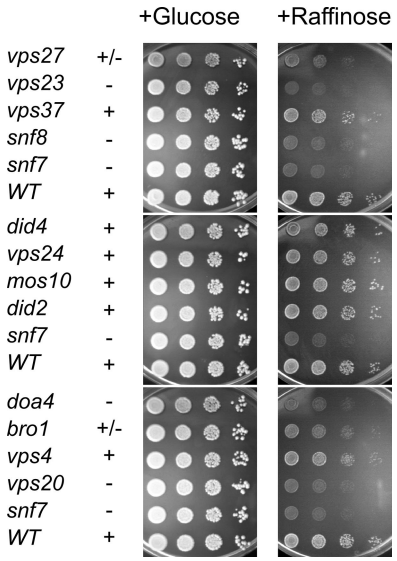


FIG. 4. Growth of "class E" mutant strains on raffinose plates. Tenfold serial dilutions of overnight cultures of different yeast strains grown in YPD medium were spotted onto YPD plates containing 2% glucose (left panels) or 2% raffinose (right panels) as the sole carbon source. Plates were incubated at 25°C for 4 days. The yeast mutants are derived from the wild-type (WT) strain JD52 and carry deletion mutations of the genes indicated. +, ±, and −, respectively, indicate growth, some growth, and no growth on raffinose plates.

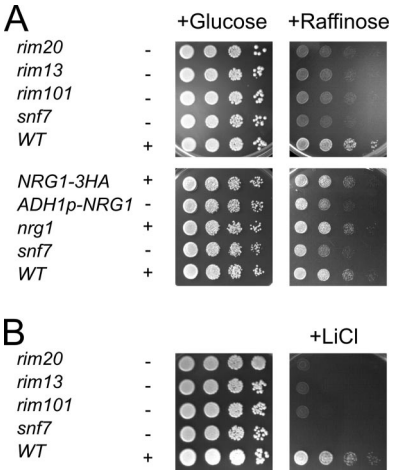


FIG. 5. Growth phenotypes of Rim101 pathway mutants. Tenfold serial dilutions of overnight cultures of different yeast strains grown in YPD medium were spotted onto YPD plates containing 2% glucose (left panels) or 2% raffinose (right panels) as the sole carbon source (A) or onto a normal YPD plate (left panel) and a YPD plate containing 0.3 M LiCl (right panel) (B). Plates were incubated at 25°C for 4 days. The yeast mutants were derived from the wild-type (WT) strain JD52 and carry deletion mutations of the genes indicated. *NRG1-3HA* represents expression of epitope-tagged Nrg1, and ADH1p-*NRG1* represents overexpression of *NRG1* from the *ADH1* promoter. +, ±, and −, respectively, indicate growth, some growth, and no growth on raffinose plates.

**Regulation of *SUC2* expression by the Rim101 pathway.** A similar dependence on ESCRT functions as observed for *SUC2* expression has been reported for the alkaline response pathway (the Rim101 pathway). In response to alkaline pH, the transcription factor Rim101 is activated by proteolytic cleavage (11). Snf7 plays a central role in this processing event by recruiting the processing factors Rim13 and Rim20 (30). Because of the similar requirements for upstream ESCRT functions (31), we examined whether *SUC2* is also a target of the Rim101 pathway by testing *rim* mutants for growth on raffinose plates (Fig. 5A). Indeed, we found that *rim13*, *rim20*, and *rim101*

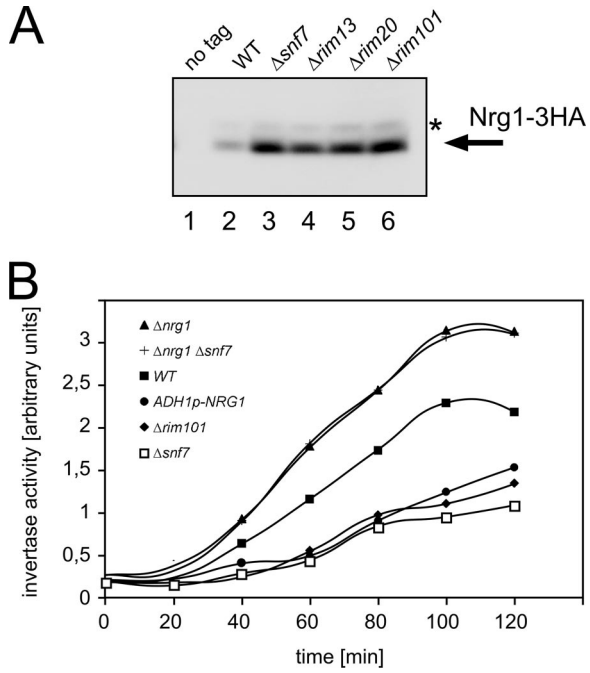


FIG. 6. Effect of Nrg1 on *SUC2* expression. (A) Expression levels of Nrg1-3HA in several yeast strains were determined by Western blotting with anti-HA antibodies. Lane 1, JD52 (wild type [WT], no tag), lane 2, RKY2176 (*SNF7*); lane 3, RKY2180 (Δ*snf7*); lane 4, RKY2284 (Δ*rim13*); lane 5, RKY2285 (Δ*rim20*); lane 6, RKY2286 (Δ*rim101*). The arrow points to the main Nrg1-3HA band; the phosphorylated form is marked with an asterisk. (B) Yeast cells pregrown in YPD medium with 5% glucose were shifted to low-glucose medium (0.1%). At time intervals after the shift to low glucose, invertase activity was determined. Strains: closed squares, JD52 (WT); open squares, RKY1852 (Δ*snf7*); closed diamonds, RKY2175 (Δ*rim101*); closed triangles, RKY2206 (Δ*nrg1*); crosses, RKY2207 (Δ*nrg1* Δ*snf7*); and closed circles, RKY2208 (*ADH1p-NRG1*).

deletion mutants are unable to grow on raffinose. This suggests that *SUC2* is regulated by the Rim101 pathway.

Several other phenotypes have been described for *rim* mutants, like cold sensitivity, sensitivity to $Na^+$ or $Li^+$ ions (30), defects in sporulation (24), and haploid-invasive growth (11). Indeed, we could show that the Δ*snf7* mutant shows the same lithium sensitivity as the *rim* mutants (Fig. 5B).

How does Rim101 regulate *SUC2* expression? Rim101 could either bind directly to the *SUC2* promoter, or it could regulate the expression of a transcription factor that binds to the *SUC2* promoter. Since there was no evidence for a direct role of Rim101 at the *SUC2* promoter, we looked for Rim101 targets that could be involved in *SUC2* regulation (9). The Rim101 target Nrg1 has been implicated before in *SUC2* regulation (32). We therefore examined the role of Nrg1 in Snf7-dependent regulation of *SUC2* expression. Nrg1 acts as a *SUC2* repressor, while Rim101 in turn represses *NRG1*. Thus, Rim101 should have a positive effect on *SUC2* transcription by lowering Nrg1 levels. In turn, Nrg1 levels should be higher in a Δ*snf7* mutant, where Rim101 activation is prevented. Indeed, we could show that the level of Nrg1 is much higher in the Δ*snf7* mutant than in the wild type (Fig. 6A). Also, a similar elevated Nrg1 expression level was observed in the *rim* mutants.

To test whether altered Nrg1 levels could explain the effect of Δ*snf7* on *SUC2* expression, induction of invertase activity after the shift to low-glucose medium was measured in various mutants (Fig. 6B). Compared to the wild type, the invertase activity in the Δ*snf7* strain after 2 h of derepression was much lower (about 30% of the wild-type level). Exactly the same level of activity was reached in a Δ*rim101* mutant and upon overexpression of *NRG1* from the *ADH1* promoter. This is consistent with the view that Δ*snf7* exerts its effect on *SUC2* by increased Nrg1 levels. Also, invertase activity was clearly higher in a Δ*nrg1* strain than in the wild type. Most interestingly, invertase activity was no longer dependent on Snf7 in the Δ*nrg1* background. Thus, Snf7 exlusively acts on *SUC2* by affecting Nrg1 levels. As expected, altered Nrg1 levels affected the growth on raffinose plates (Fig. 5A). While the Δ*nrg1* mutant grew like the wild type, the *NRG1*-overexpressing strain had a growth defect similar to that of the Δ*snf7* mutant.

## DISCUSSION

In this report, we explore the molecular basis for the sucrose-nonfermenting phenotype of *snf7* mutants. We demonstrate that the ESCRT-III protein Snf7 mediates high-level expression of the *SUC2* gene via the Rim101 pathway.

Our Northern blotting experiments provide evidence that Snf7 is involved in the regulation of *SUC2* transcript levels. One potential target for Snf7 could be glucose signaling at the *SUC2* promoter. Upon glucose limitation, the Mig1 repressor, which represses *SUC2* expression on high glucose, is inactivated by phosphorylation (26). This Mig1 phosphorylation, however, was not affected in the Δ*snf7* mutant. Thus, Snf7 appears to affect events at the *SUC2* promoter independent of Mig1. This notion is also supported by earlier findings that galactose utilization, which is also under Mig1 control, is not affected in *snf7* mutants (28).

From our data, we conclude that Snf7 influences *SUC2* expression by regulating the level of Nrg1, a transcription factor already implicated in *SUC2* regulation. *NRG1* transcription is negatively controlled by the transcription factor Rim101 (9). This transcription factor in turn is activated by proteolytic cleavage in response to alkaline pH (11). Snf7 appears to be an integral part of the complex involved in Rim101 cleavage consisting of the Bro1 homologue Rim20 and the calpain-like protease Rim13 (30). The effect of Snf7 on *SUC2* expression can be completely accounted for by its effect on Nrg1 levels. This notion is supported by the following findings: (i) deletion of *RIM101* or overexpression of *NRG1* from the *ADH1* promoter leads to the same *SUC2* expression level as deletion of *SNF7* and (ii) Snf7 is dispensable for *SUC2* expression in an *NRG1* deletion background. This implies that the RIM101 pathway is fully active at the pH of our growth media used for the invertase assays. Indeed, we found that Rim101 is completely processed under these conditions (data not shown).

*SUC2* shows a biphasic transcription profile after derepression (5). After an initial burst of transcription, transcript levels drop and then rise again. In the Δ*snf7* mutant, the initial burst of transcription seems to be missing. Since the only role of Snf7 in *SUC2* expression is to modulate Nrg1 levels, the release from Nrg1 repression appears to be defective in the Δ*snf7* mutant. How Nrg1 repression is released after the shift to low

glucose is not known, but apparently inactivation is counteracted by high Nrg1 levels. It has been reported that Nrg1 becomes phosphorylated by protein kinase CK2 after exposure to various stress conditions, among them the shift to low glucose (4). The consequences of this modification, however, remained unclear. We could also detect phosphorylation of Nrg1 (Fig. 6A), but in our hands, there was no significant change in phosphorylation upon shift to low glucose or in the Δ*snf7* mutant compared to the wild type (data not shown). Thus, how exactly Nrg1 repression is released after the shift to low glucose remains elusive. In any case, at later time points after derepression, Nrg1 does not act any longer as a repressor irrespective of the amounts of Nrg1 present.

It is not immediately obvious why the *SUC2* gene, which is mainly controlled by the carbon source, should be under the control of the alkaline response pathway. One possible explanation could be that carbon source utilization is somehow connected to the pH of the growth medium. Indeed, it has been reported that growth on high glucose concentrations lowers the pH, while growth on a poor carbon source, like acetate, results in a pH increase (11). Thus, active growth, independent from the carbon source used, would exert a negative effect on *SUC2* expression via lowered pH and a less active RIM101 pathway.

Alternatively, the RIM101 pathway could have other roles in gene expression beyond pH control. In fact, the association between the RIM101 pathway and pH control in *Saccharomyces cerevisiae* is not as tight as in *Aspergillus nidulans*, where this system was initially discovered (9). By macroarray analysis, alkaline-induced genes in *S. cerevisiae* were identified (10). Only some of these genes turned out to be regulated by Rim101. In addition, some Rim101 target genes were still pH regulated in the presence of the constitutively active Rim101-531 mutant protein. This suggests that there are additional mechanisms of pH control in *S. cerevisiae*. Furthermore, *rim* mutants show many phenotypes, like cold sensitivity, sensitivity to $Na^+$ or $Li^+$ ions (30), defects in sporulation (24), and haploid-invasive growth (11), which may not be directly linked to pH control.

*SUC2* is not the only yeast gene that is controlled by both Mig1 (and/or the homologous protein Mig2) and by Nrg1 (and/or the homologous protein Nrg2). For instance, *ENA1*, coding for the $Na^+$-ATPase, is similarly regulated by Nrg1 and Mig2 (and additional factors) (20). In addition, a database query in the YEASTRACT database (25) revealed 40 genes whose expression is affected by both Mig1/2 and Nrg1/2. Thus, for a certain set of genes, it appears to be beneficial to link carbon source control via Mig1/2 and stress signaling via Nrg1/2.

Proteolytic activation of Rim101 is connected to a functional ESCRT pathway (31). The current view is that the protein complexes of the ESCRT pathway are assembled at the endosomal membrane in a fixed order and that each complex assists in recruitment of the following complex (22). In line with previous findings, we found that the components placed "upstream" of the Snf7/Vps20 subcomplex in this assembly pathway are required for optimal growth on raffinose (i.e., full *SUC2* expression), while the "downstream" components appear to be dispensable. From this, it can be concluded that the main function of the ESCRT pathway, with respect to Rim101 processing, is to bring Snf7/Vps20 to the membrane. Membrane association appears to be a prerequisite for assembly of an active Snf7/Rim20/Rim13 processing complex.

However, there are some conflicts with published reports as to the contribution of some of the "class E" functions (Vps27, Vps37, Bro1, and Doa4) to Rim101 activation (21, 31). Basically, our results are in agreement with the study by Rothfels et al. (21). We find that Vps37 is not required for growth on raffinose, while Doa4 is required and Bro1 is partially required. It is unclear why some upstream components of the ESCRT pathway (like Vps37 and maybe Vps27) should not be required for Rim101 activation. However, it is conceivable that the requirements for Rim101 activation may not be as stringent as the requirements for the proper functioning of the ESCRT pathway.

Why Rim101 processing only occurs at the membrane is at present unclear. Perhaps, membrane association is necessary to integrate signaling events with Rim101 processing.

## ACKNOWLEDGMENTS

We thank Karin Krapka for assistance with some of the experiments. This work was supported by the DFG grant Ko 963/5-1.

## REFERENCES

1. **Amerik, A. Y., J. Nowak, S. Swaminathan, and M. Hochstrasser.** 2000. The Doa4 deubiquitinating enzyme is functionally linked to the vacuolar protein-sorting and endocytic pathways. Mol. Biol. Cell **11:**3365–3380.
2. **Babst, M., D. J. Katzmann, E. J. Estepa-Sabal, T. Meerloo, and S. D. Emr.** 2002. ESCRT-III: an endosome-associated heterooligomeric protein complex required for MVB sorting. Dev. Cell **3:**271–282.
3. **Babst, M., B. Wendland, E. J. Estepa, and S. D. Emr.** 1998. The Vps4p AAA ATPase regulates membrane association of a Vps protein complex required for normal endosome function. EMBO J. **17:**2982–2993.
4. **Berkey, C. D., and M. Carlson.** 2006. A specific catalytic subunit isoform of protein kinase CK2 is required for phosphorylation of the repressor Nrg1 in *Saccharomyces cerevisiae*. Curr. Genet. **50:**1–10.
5. **Geng, F., and B. C. Laurent.** 2004. Roles of SWI/SNF and HATs throughout the dynamic transcription of a yeast glucose-repressible gene. EMBO J. **23:**127–137.
6. **Howard, T. L., D. R. Stauffer, C. R. Degnin, and S. M. Hollenberg.** 2001. CHMP1 functions as a member of a newly defined family of vesicle trafficking proteins. J. Cell Sci. **114:**2395–2404.
7. **Jiang, R., and M. Carlson.** 1997. The Snf1 protein kinase and its activating subunit, Snf4, interact with distinct domains of the Sip1/Sip2/Gal83 component in the kinase complex. Mol. Cell. Biol. **17:**2099–2106.
8. **Kranz, A., A. Kinner, and R. Kölling.** 2001. A family of small coiled-coil-forming proteins functioning at the late endosome in yeast. Mol. Biol. Cell **12:**711–723.
9. **Lamb, T. M., and A. P. Mitchell.** 2003. The transcription factor Rim101p governs ion tolerance and cell differentiation by direct repression of the regulatory genes *NRG1* and *SMP1* in *Saccharomyces cerevisiae*. Mol. Cell. Biol. **23:**677–686.
10. **Lamb, T. M., W. Xu, A. Diamond, and A. P. Mitchell.** 2001. Alkaline response genes of *Saccharomyces cerevisiae* and their relationship to the *RIM101* pathway. J. Biol. Chem. **276:**1850–1856.
11. **Li, W., and A. P. Mitchell.** 1997. Proteolytic activation of Rim1p, a positive regulator of yeast sporulation and invasive growth. Genetics **145:**63–73.
12. **Longtine, M. S., A. McKenzie III, D. J. Demarini, N. G. Shah, A. Wach, A. Brachat, P. Philippsen, and J. R. Pringle.** 1998. Additional modules for versatile and economical PCR-based gene deletion and modification in *Saccharomyces cerevisiae*. Yeast **14:**953–961.
13. **Luhtala, N., and G. Odorizzi.** 2004. Bro1 coordinates deubiquitination in the multivesicular body pathway by recruiting Doa4 to endosomes. J. Cell Biol. **166:**717–729.
14. **Nehlin, J. O., and H. Ronne.** 1990. Yeast *MIG1* repressor is related to the mammalian early growth response and Wilms' tumour finger proteins. EMBO J. **9:**2891–2898.
15. **Neigeborn, L., and M. Carlson.** 1984. Genes affecting the regulation of *SUC2* gene expression by glucose repression in *Saccharomyces cerevisiae*. Genetics **108:**845–858.
16. **Nikko, E., and B. André.** 2007. Evidence for a direct role of the Doa4 deubiquitinating enzyme in protein sorting into the MVB pathway. Traffic **8:**566–581.

17. **Nikko, E., A. M. Marini, and B. André.** 2003. Permease recycling and ubiquitination status reveal a particular role for Bro1 in the multivesicular body pathway. J. Biol. Chem. **278:**50732–50743.
18. **Odorizzi, G., M. Babst, and S. D. Emr.** 1998. Fab1p PtdIns(3)P 5-kinase function essential for protein sorting in the multivesicular body. Cell **95:**847–858.
19. **Odorizzi, G., D. J. Katzmann, M. Babst, A. Audhya, and S. D. Emr.** 2003. Bro1 is an endosome-associated protein that functions in the MVB pathway in *Saccharomyces cerevisiae*. J. Cell Sci. **116:**1893–1903.
20. **Platara, M., A. Ruiz, R. Serrano, A. Palomino, F. Moreno, and J. Arino.** 2006. The transcriptional response of the yeast Na(+)-ATPase *ENA1* gene to alkaline stress involves three main signaling pathways. J. Biol. Chem. **281:**36632–36642.
21. **Rothfels, K., J. C. Tanny, E. Molnar, H. Friesen, C. Commisso, and J. Segall.** 2005. Components of the ESCRT pathway, *DFG16*, and *YGR122w* are required for Rim101 to act as a corepressor with Nrg1 at the negative regulatory element of the *DIT1* gene of *Saccharomyces cerevisiae*. Mol. Cell. Biol. **25:**6772–6788.
22. **Saksena, S., J. Sun, T. Chu, and S. D. Emr.** 2007. ESCRTing proteins in the endocytic pathway. Trends Biochem. Sci. **32:**561–573.
23. **Schmitz, H. P., A. Lorberg, and J. J. Heinisch.** 2002. Regulation of yeast protein kinase C activity by interaction with the small GTPase Rho1p through its amino-terminal HR1 domain. Mol. Microbiol. **44:**829–840.
24. **Su, S. S., and A. P. Mitchell.** 1993. Identification of functionally related genes that stimulate early meiotic gene expression in yeast. Genetics **133:**67–77.
25. **Teixeira, M. C., P. Monteiro, P. Jain, S. Tenreiro, A. R. Fernandes, N. P. Mira, M. Alenquer, A. T. Freitas, A. L. Oliveira, and I. Sa-Correia.** 2006. The YEASTRACT database: a tool for the analysis of transcription regulatory associations in *Saccharomyces cerevisiae*. Nucleic Acids Res. **34:**D446–D451.
26. **Treitel, M. A., S. Kuchin, and M. Carlson.** 1998. Snf1 protein kinase regulates phosphorylation of the Mig1 repressor in *Saccharomyces cerevisiae*. Mol. Cell. Biol. **18:**6273–6280.
27. **Tu, J., L. G. Vallier, and M. Carlson.** 1993. Molecular and genetic analysis of the *SNF7* gene in *Saccharomyces cerevisiae*. Genetics **135:**17–23.
28. **Vallier, L. G., and M. Carlson.** 1991. New *SNF* genes, *GAL11* and *GRR1* affect *SUC2* expression in *Saccharomyces cerevisiae*. Genetics **129:**675–684.
29. **Vignali, M., A. H. Hassan, K. E. Neely, and J. L. Workman.** 2000. ATP-dependent chromatin-remodeling complexes. Mol. Cell. Biol. **20:**1899–1910.
30. **Xu, W., and A. P. Mitchell.** 2001. Yeast PalA/AIP1/Alix homolog Rim20p associates with a PEST-like region and is required for its proteolytic cleavage. J. Bacteriol. **183:**6917–6923.
31. **Xu, W., F. J. Smith, Jr., R. Subaran, and A. P. Mitchell.** 2004. Multivesicular body-ESCRT components function in pH response regulation in *Saccharomyces cerevisiae* and *Candida albicans*. Mol. Biol. Cell **15:**5528–5537.
32. **Zhou, H., and F. Winston.** 2001. *NRG1* is required for glucose repression of the *SUC2* and *GAL* genes of *Saccharomyces cerevisiae*. BMC Genet. **2:**5.